Available online at www.sciencedirect.com
SCIENCE DIRECT
Aerospace Science and Technology 10 (2006) 435–441
Aerospace Science and Technology
www.elsevier.com/locate/aescte

Flutter control of a composite plate with piezoelectric multilayered actuators

S. Raja [a,*], A.A. Pashilkar [b], R. Sreedeep [a], J.V. Kamesh [c]

[a] *Aeroelasticity and Smart Structures Group, Structures Division, National Aerospace Laboratories (CSIR), Bangalore 560017, India*
[b] *Flight Mechanics and Controls Division, National Aerospace Laboratories (CSIR), Bangalore 560017, India*
[c] *Aeronautical Development Agency, Bangalore 560037, India*

Received 11 August 2005; received in revised form 28 December 2005; accepted 5 January 2006

Available online 14 February 2006

Abstract

Active flutter velocity enhancement scheme is presented for lifting surfaces, employing Linear Quadratic Gaussian based multi-input multi-output controller with multilayered piezoelectric actuators. To numerically test the developed concept, a composite plate wing, surface bonded with eight piezoelectric bender actuators and sensors has been considered. A modal flutter control model is formulated in state-space domain using coupled piezoelectric finite element procedures along with unsteady aerodynamics and optimal control theory. The bending – torsion flutter instability has been actively postponed from 44.13 to 55.5 m/s using the energy imparted by the multilayered piezoelectric actuators. As the power requirement by these actuators is comparatively very low with respect to stack actuators, they can be employed in an integrated form to develop active lifting surfaces for real time applications.

Keywords: Flutter; Active flutter control (AFC); Piezoelectricity; Smart structures

1. Introduction

Flutter is a catastrophic dynamic aeroelastic phenomenon that can occur at speed, which is expected to be 1.2 times the diving velocity for an aircraft to ensure flight safety. Beyond flutter velocity, the aeroelastic system actually extracts energy from the free stream flow to develop a divergent response. It is to be noted that flutter is usually the resultant of coupling between two or more structural modes, influenced by unsteady aerodynamics. The flutter speed actually poses constraints on aircraft design, which brings limitation in the flight envelope. Active and passive control methods have been developed in the last three decades and applied to enhance the flutter velocity. Active methods are more robust and utilises plant information effectively to account for uncertainties in real time (*variable gain controller*) or off line (*constant gain controller*).

Design of active flutter suppression systems has been attempted, following the classical technologies such as Root-Locus Method [1,2], Frequency Response Method [3] and also the modern Optimal Control Theory. Techniques such as Nissim's Aerodynamic Energy Concept [4] and the Method of Fictitious Structural Modifications [5] have also been applied. Several researchers have used optimal regulator theory to design the active flutter suppression systems [6–10]. Nam and Kim [11] have developed an active control system to study flutter suppression of a composite wing using segmented piezoelectric actuators. Optimal output feedback control (LQR) has been used with optimisation technique to locate the actuators in control scheme. A 49% flutter velocity enhancement has been reported by using piezoelectric actuation. Barker et al. [12] have introduced a control theory based on gain-scheduled Linear Fractional Transformation (LFT) for a wind tunnel model. The control concept is implemented successfully for a wide range of operating conditions to achieve vibration attenuation. A comparative study has also been made on an optimised linear controller with LFT based control scheme, which has shown superior performance.

Friedmann and Presente [13] have proposed a new approach that is capable of providing useful scaling information on hinge moment and power requirement for flutter suppression. Recently Newsom has reported a general design methodology to

* Corresponding author. Tel.: +91 (80) 25086209.
E-mail address: raja@css.cmmacs.ernet.in (S. Raja).

1270-9638/$ – see front matter
doi:10.1016/j.ast.2006.01.003

Nomenclature

ρ	density
σ	stress
D	electric displacement
E	electric field
f_s	surface traction
q	surface charge
$[c]$	elastic constant
ε	strain
$[d]$	piezoelectric constant
$[\kappa]$	dielectric constant
$[M_{uu}]$	mass matrix
$[D_{uu}]$	damping matrix
$[K_{uu}]$	stiffness matrix
f_d	disturbance force
ϕ	electric potential
ϕ_a	actuator voltage
ϕ_s	sensor voltage
$[K_{u\phi}]$	actuator influence matrix
$[K_{\phi u}]$	sensor influence matrix
$[K_{\phi\phi}]$	capacitance matrix
$u, \ddot{u}$	displacement and acceleration
$\bar{Q}(k)$	complex generalized aerodynamic influence matrix in modal coordinates
k	reduced frequency
$[\bar{M}_{uu}]$	modal mass matrix
$[\bar{D}_{uu}]$	modal damping matrix
$[\bar{K}_{uu}]$	modal stiffness matrix
U	velocity of airflow
$\bar{u}, \dot{\bar{u}}$	modal displacement, modal velocity
ψ	modal matrix containing eigenvectors of conservative elastic system
b	reference semi-chord
ω	frequency in rad/s
A	system matrix
B, B_d	control input matrices
β	process noise
C	measurement matrix
χ	measurement noise
Q, R	state & control weighting matrices
K_e	estimator gain matrix
K_c	feedback gain matrix
S_e, S_c	steady state solutions
f_a	actuator force
u_d	disturbance input
LQG	Linear Quadratic Gaussian
LQR	Linear Quadratic Regulator

develop active control laws for aeroelastic control applications, employing state-space approach [14]. A modern system identification technique is used to develop an equivalent linear model from the non-linear simulation results. LQG design technique is then adopted in the development of control laws with non-linear aeroelasticity.

Jennifer Heeg has studied the capabilities of piezoelectric plate actuators to suppress flutter of a two-degrees of freedom flexible wind tunnel model [15]. The model has been designed to flutter within the test envelope of the tunnel. An aeroservoelastic analytical model is then constructed using finite element and aeroelastic analyses tools. Further experiments have been conducted using digital control scheme to demonstrate the efficiency of piezoelectric actuators in flutter control mechanism. Döngi et al. [16] have presented a finite element method based numerical solution for flutter suppression of adaptive panel with self-sensing piezoelectric actuators in high supersonic flow. A control approach based on output feedback using collocated piezoelectric actuators is introduced with a simple analog circuit.

Active control system having piezoelectric sensors, actuators and an associated controller (analog or digital) can be employed to bring down the vibration level of elastic modes. Sensors are employed to sense the structural responses due to external disturbances and feedback the response signals via controller to actuators. Piezoelectric actuators are able to change shape, stiffness, damping and/or other mechanical characteristics of vibrating system suitably to minimize the undesired effect. Piezoelectric actuators are being constructed in multilayered form to enhance the actuation power; for example multilayered benders (MLB), stack.

There have been significant amount of literatures reported in the area of active vibration control of flexible structures, using piezoelectric materials; however only a limited number of research works has been carried out in the field of dynamic aeroelastic control. Also, the reported studies on flutter suppression mainly have employed PZT wafers or patches; the efficiency of real time actuators like multilayered PZT actuators in controlling the aeroelastic instability has not been addressed properly so far (to the best of authors knowledge). The present study is aimed to use the multilayered PZT benders as distributed actuators and PZT wafers as feedback sensors to solve aeroelastic closed loop flutter of a cantilever composite plate wing using LQG control. The advantages of using these actuators on lifting surfaces are easy integration and low voltage (0 to 60 VDC; ±30 VAC), low current requirements unlike stack actuators. Each actuator is capable of developing 0.6 N block force and 1.0 mm free deflection. As a model problem, an active composite plate representing a fixed-free wing configuration is idealized with GFRP material. The plate is made active by surface bonding eight PZT co-fired multilayered benders as actuators (Piezomechanik®, GmbH) on the top and eight PZT wafers are collocated at the bottom side for sensing purpose in the feedback control (refer to Fig. 1). The active plate dynamics have been modelled using a field consistent four noded piezo-elastic plate bending element. The unsteady aerodynamic calculations

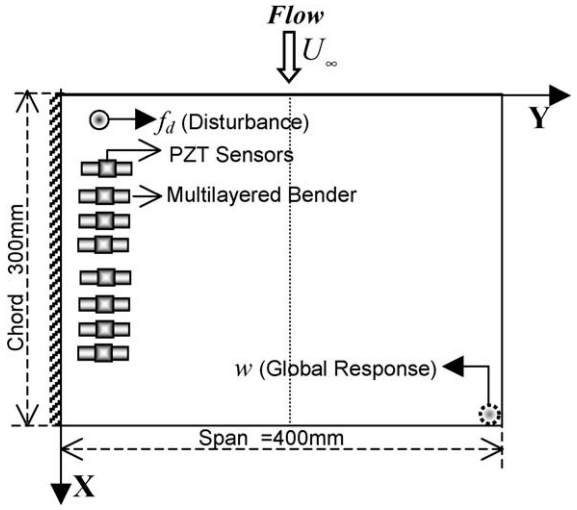

Fig. 1. Active composite plate.

are done in MSC/NASTRAN® to obtain the generalized aerodynamic forces and the same are used in the open and closed loop flutter analyses by State-Space Approach (SSA).

2. Plant modeling

The elastic system consists of a GFRP plate and eight collocated actuator-sensor pairs. The multi-functional actuators and sensors are modeled as an additional layer in active laminate to capture their elastic contribution. The dynamic analysis is subsequently carried out in NASTRAN® (CQUAD4) to obtain the natural frequencies and mode shapes. To perform an electro-mechanical analysis on the active plate, a coupled four noded quadrilateral piezo-elastic plate bending element (NAL-QUAD4E) is developed. Using the virtual work principle, the coupled piezo-elastic energy is derived as

$$\int_V \big(\rho\{\ddot{u}\}\{\delta u\} + \{\sigma\}\{\delta\varepsilon\} - \{D\}\{\delta E\}\big)\,\mathrm{d}v = \int_S \{f_s\}\{\delta u\}\,\mathrm{d}s + \int_S q\delta\phi\,\mathrm{d}s. \quad (1)$$

The piezo-elastic coupling is introduced through constitutive relations to expand the above Eq. (1), to arrive at the necessary equilibrium equations and boundary conditions:

$$\{\sigma\} = [c]\{\varepsilon\} - [d]\{E\},$$
$$\{D\} = [d]^{\mathrm{T}}\{\varepsilon\} + [\kappa]\{E\}. \quad (2)$$

Further, the obtained equilibrium equation is approximated using isoparametric shape functions to derive a four noded piezo-elastic plate bending element [17]. The final discrete form of equilibrium equations are given by

$$[M_{uu}]\{\ddot{u}\} + [K_{uu}]\{u\} = \{f_d\} - [K_{u\phi}]\{\phi_a\},$$
$$[K_{\phi u}]\{u\} + [K_{\phi\phi}]\{\phi_s\} = 0. \quad (3)$$

The subscripts ‘a’, ‘s’ denote actuator and sensor, respectively.

Table 1
Comparison of frequencies (Hz)

Mode order	NAL-QUAD4E	MSC/NASTRAN®_CQUAD4
1	9.36	9.34
2	19.20	19.23
3	46.70	46.16

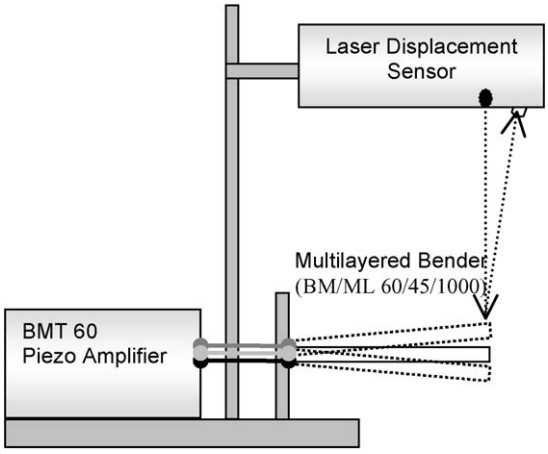

(a)

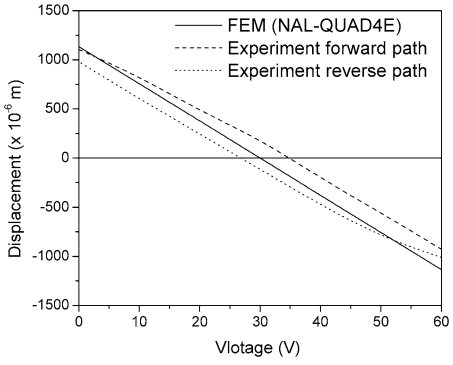

(b)

Fig. 2. Experimental validation for multilayered bender. (a) Experimental setup. (b) Static deflection behavior.

The developed element has both mechanical and electric field variables, which facilitate to impose specified displacements and electric potentials. Further, this coupled element’s performance is thoroughly validated with CQUAD4 of NASTRAN® to predict the static and dynamic behavior of laminated composite plates. In Table 1, the elastic frequencies predicted by NAL-QUAD4E and CQUAD4 of NASTRAN® are presented, basically to show the structural dynamics are similarly captured by both analyses. The system parameters such as mass, stiffness, piezoelectric coupling and capacitance matrices of active devices (actuator/sensor) are generated from smart finite element analysis using NAL-QUAD4E element.

The multilayered benders (MLB) are made by co-firing process, each layer having thickness of around 25–40 μm (dimension 45 × 11 × 0.5 mm). However, these bender actuators are modeled as bimorph benders with equivalent electric field strength to generate the same induced strain actuation like

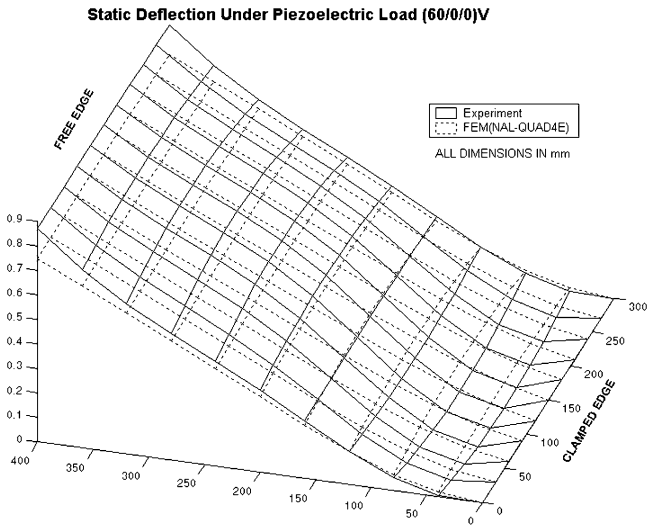

Fig. 3. Static deflection of active plate under piezoelectric loading.

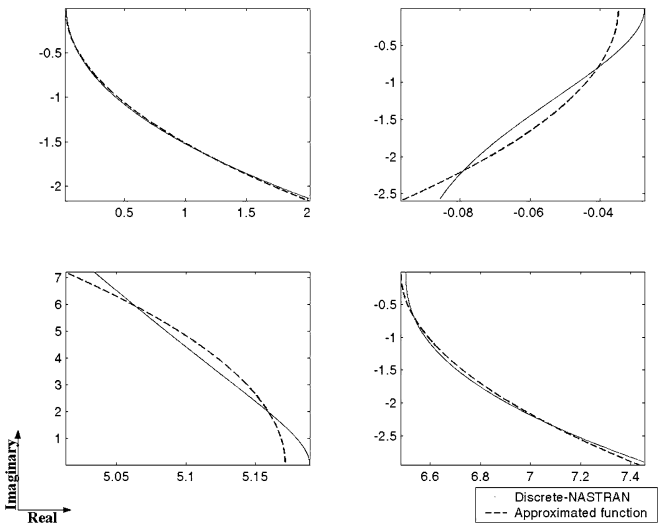

Fig. 4. Approximated generalized air loads.

multi-layered configuration. To fully qualify the MLB actuator for active flutter control (AFC) application, experiments are conducted to measure the free deflection using a laser sensing system (see Fig. 2(a)). The MLB actuator has a three pole electrical configuration, namely fixed: 60 V, variable: 0 to 60 (VDC) or ±30 (VAC) and ground. The bender is modeled using NAL-QUAD4E element for a variable voltage 0 to 60 V and the numerical simulations are compared with experimental results (in Fig. 2(b)).

The potential of the actuators to deflect the composite plate is numerically captured and the results are verified with experiments (refer to Fig. 3). A single channel laser sensing system is used to measure the piezoelectrically developed deflection at various nodal points. This exercise has helped to check the smart structure modeling, further to ensure the aeroelastic system is correctly idealized.

3. Aerodynamic load approximation

It has been already shown that both NAL-QUAD4E and CQUAD4 (NASTRAN®) are closely predicting the normal modes of the active composite plate, therefore the flexible aerodynamic loads estimated from NASTRAN® can be employed directly with NAL-QUAD4E to develop the necessary state-space model for the design of active flutter suppression system.

The unsteady aerodynamic calculation is done using a linear two dimensional aerodynamic theory (*Doublet-Lattice Method* in NASTRAN®) for the active flutter control studies. In this approach, a flat plate represents the lifting surface, where the thickness effect is neglected. The closed loop flutter calculation with active control involves aeroelastic energy (aerodynamic and structural) interaction with control energy. This demands a mathematical model of active plate with coupled actuator/sensor influence matrices plus structural matrices in a platform where control design can be performed. A State Space Approach (SSA) is most suitable to meet this requirement in MATLAB/SIMULINK® environment.

The generalized unsteady aerodynamic loads in modal domain for a range of reduced frequencies (k) and a Mach number (M) are obtained using *Direct Matrix Abstraction Programme* (DMAP) from NASTRAN®. The flight conditions are sea level atmospheric ($\rho = 1.225$ kg/m^3) and low subsonic velocity regime. These generalized air loads are discrete in nature. Therefore, the discrete load coefficients have been made as continuous function for flutter control application by approximating the air load coefficients through *rational polynomials* in *Laplace* domain.

To build an aeroelastic plant in SSA, the discrete air loads obtained using NASTRAN® have been represented as a continuous function in *Laplace* domain [18]:

$$\bar{Q}(k) = A_0 + A_1(ik) + A_2(ik)^2, \tag{4}$$

where A_0, A_1 and A_2 are the approximation coefficients, defining A_0 is equivalent aerodynamic stiffness, A_1 is equivalent aerodynamic damping, A_2 is equivalent aerodynamic inertia.

The above approximation coefficients are obtained in matrix form by least square error technique, where $\bar{Q}(k)$ is calculated at discrete values of reduced frequencies from NASTRAN®. Typical plots of the approximated aerodynamic loads for the first two elastic modes are presented in the Fig. 4.

4. Open loop flutter estimation

An open loop flutter analysis is performed by considering two modes only (bending and torsion). The active plate structural matrices obtained from NAL-QUAD4E are first converted into modal form. The approximated air load coefficients estimated in modal domain are used along with structural matrices to build a state-space model to conduct open loop flutter analysis. The formulation is briefly presented here.

Open loop flutter solution in 's' domain is expressed as follows:

$$\left([\bar{M}_{uu}]s^2 + [\bar{D}_{uu}]s + \frac{1}{2}\rho U^2\big[\bar{Q}(k)\big] + [\bar{K}_{uu}]\right)\{\bar{u}\} = 0, \tag{5}$$

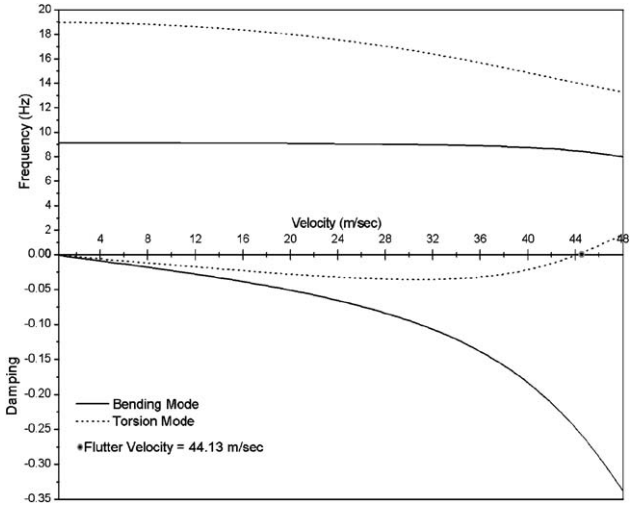

Fig. 5. Open loop flutter characteristics (SSA).

Table 2
Open loop flutter velocity comparison with NASTRAN®

	Flutter velocity [m/s]	Flutter frequency [HZ]
NASTRAN	43.81	14.026
SSA	44.13	14.034
% deviation	0.73	0.014

$$k = \frac{\omega b}{U}, \qquad s = i\omega, \qquad ik = \frac{sb}{U},$$
$$\bar{M}_{uu} = \psi^{\mathrm{T}} M_{uu} \psi,$$
$$\bar{D}_{uu} = \psi^{\mathrm{T}} D_{uu} \psi,$$
$$\bar{K}_{uu} = \psi^{\mathrm{T}} K_{uu} \psi.$$

Above second order equation can be written as two first order equations in state-space form without structural damping using a new state vector $\{x\} = \{x_1, x_2\}^{\mathrm{T}} = \{\bar{u}, \dot{\bar{u}}\}^{\mathrm{T}}$, where x_1 and x_2 are modal displacement and modal velocity, respectively.

A complex eigenvalue problem is then formed and solved for a range of velocities.

$$\begin{Bmatrix} \dot{x}_1 \\ \dot{x}_2 \end{Bmatrix} = \begin{bmatrix} 0 & I \\ -\left(\frac{[\bar{K}_{uu}] + \frac{1}{2}\rho U^2 [A_0]}{[\bar{M}_{uu}] + \frac{1}{2}\rho b^2 [\mathrm{A}_2]}\right) & -\left(\frac{\frac{1}{2}\rho U b [A_1]}{[\bar{M}_{uu}] + \frac{1}{2}\rho b^2 [A_2]}\right) \end{bmatrix} \times \begin{Bmatrix} x_1 \\ x_2 \end{Bmatrix}. \tag{6}$$

The complex roots of the solution to Eq. (6), indicate the damping and frequency behavior of the active composite plate, using which the flutter velocity and frequency are estimated (refer to Fig. 5). The flutter analysis results of state-space approach have been compared with NASTRAN® analysis in Table 2. The open loop flutter estimation by state-space approach appears to be reasonable.

5. Active control strategy

Eight actuators and sensors have been employed in a feedback configuration with LQG methodology to develop active flutter control concept. The aeroelastic system is modeled for different velocities, ranging from 10 m/s to flutter velocity (44.13 m/s). The actuators and sensors are located at maximum strain energy places in the structure with an intention of maximizing their effectiveness. Also shown in the Fig. 1 is an input disturbance force f_d near the root of the plate. This disturbance point is used to impart an impulse to the plate and study the aeroelastic instability with and without the control system present. To study the response of the structure, a fictitious observation point has been created in the mathematical model near the right hand bottom corner of the plate. It is noted that the point of interest (w) is different from the location of the piezoelectric sensors used for feedback control. Similarly the disturbance point is different from the piezoelectric actuators. The primary aim of the active control system design is to suppress f_d to w response. This general problem formulation can be represented in a block diagram form as shown in Fig. 6. It is seen that to account for effects of digital sampling, a delay (5 ms) has been introduced in the feedback loop. The actuator voltages are also limited to ±30 Volts as shown by the signal limiter block after the feedback controller. The delay is taken into account in calculating the loop stability margins and in the simulation responses.

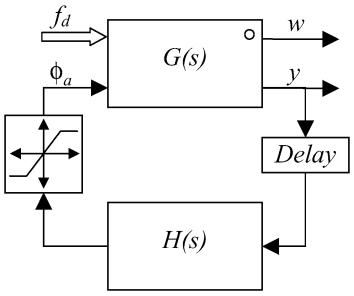

Fig. 6. Block diagram form of the plant $G(s)$ with feedback control $H(s)$.

The piezoelectric sensors only measure a signal proportional to position. The main intention of the flutter suppression controller is to improve the damping of the modes participating in the flutter. The most effective feedback to change the system damping is the velocity. Therefore, a Kalman filter is used to synthesize the velocity information from displacement measurements. The (modal) state estimation problem consists of obtaining the state of a system given its (measured) outputs and known inputs in the presence of process noise (β) and measurement noise (χ).

$$\dot{x} = Ax + B\phi_a + \beta,$$
$$y = Cx + \chi. \tag{7}$$

This problem has a general solution for linear systems. It can be shown [19] that the optimal estimator consists of a dynamic filter which receives the plant known inputs and measured outputs and computes an optimal estimate of the states. It can be thought of as a two-step process a prediction followed by a correction. The prediction process consists of the nominal open loop mathematical model of the plant. The output of prediction is compared with the measured plant outputs and a correction term applied to the state derivative with the estimator gain K_e.

$$K_e = S_e C^{\mathrm{T}} R^{-1},$$
$$A S_e + S_e A^{\mathrm{T}} - S_e C^{\mathrm{T}} R^{-1} C S_e + Q = 0. \tag{8}$$

The estimator resulting from the optimal state estimation problem is affected by noise from two sources i.e. the process noise (β) entering the system via the state equations and the measurement noise (χ). The controller then consists of two parts, i.e. the first is the estimator and the second part is the state feedback gain matrix K_c. The separation principle allows the control design also to be decomposed into two parts without losing optimality.

The motivation to utilize a model-based multivariable control approach (Multi Input Multi Output: MIMO) lies in the limitations of SISO methods (PID) in coordinating different inputs and outputs. The principle advantage of a MIMO design technique is the ability to find the full control gain matrix for the plant which exploits the inherent input-output couplings in the plant. Nevertheless, robustness of the design still remains an issue to be addressed. The LQR design formulates the control design problem in terms of an optimized cost function, consisting of weighted sum of the states and the control effort:

$$\min_{x = Ax + B\phi_a} J = \int_0^t \left(x^{\mathrm{T}} Q x + \phi_a^{\mathrm{T}} R \phi_a \right) \mathrm{d}t. \tag{9}$$

The optimal regulator gains for the system are given by

$$K_c = R^{-1} B^{\mathrm{T}} S_c. \tag{10}$$

'S_c' is the steady state solution, obtained by solving the ARE,

$$A S_c + S_c A^{\mathrm{T}} - S_c B^{\mathrm{T}} R^{-1} B S_c + Q = 0. \tag{11}$$

6. Closed loop flutter estimation with LQG control (simulation results)

Smart aeroelastic system is built by combining elastic, piezoelectric and aerodynamic system matrices.

The closed loop system equation can then be expressed as follows:

$$\left[[\bar{M}_{uu}] + \frac{1}{2}\rho b^2 [A_2] \right] \dot{x}_2 + \frac{1}{2}\rho U b [A_1] x_2 + \left([\bar{K}_{uu}] + \frac{1}{2}\rho U^2 [A_0] \right) x_1 = f_a + f_d \tag{12}$$

where $f_a = -\bar{K}_{u\phi}.\phi_a$, $f_d = B_d.u_d$.

The smart aeroelastic system in its final state-space form is obtained as

$$\begin{Bmatrix} \dot{x}_1 \\ \dot{x}_2 \end{Bmatrix} = \begin{bmatrix} 0 & I \\ -\left(\frac{[\bar{K}_{uu}] + \frac{1}{2}\rho U^2 [A_0]}{[\bar{M}_{uu}] + \frac{1}{2}\rho b^2 [A_2]} \right) & -\left(\frac{\frac{1}{2}\rho U b [A_1]}{[\bar{M}_{uu}] + \frac{1}{2}\rho b^2 [A_2]} \right) \end{bmatrix} \begin{Bmatrix} x_1 \\ x_2 \end{Bmatrix} + \begin{bmatrix} 0 & 0 \\ \left(\frac{\bar{K}_{u\phi}}{[\bar{M}_{uu}] + \frac{1}{2}\rho b^2 [A_2]} \right) & \left(\frac{B_d}{[\bar{M}_{uu}] + \frac{1}{2}\rho b^2 [A_2]} \right) \end{bmatrix} \begin{Bmatrix} \phi_a \\ u_d \end{Bmatrix},$$

$$y = [\bar{K}_{\phi u}\ 0] \begin{Bmatrix} x_1 \\ x_2 \end{Bmatrix},$$
$$(\phi_a = -K_c x). \tag{13}$$

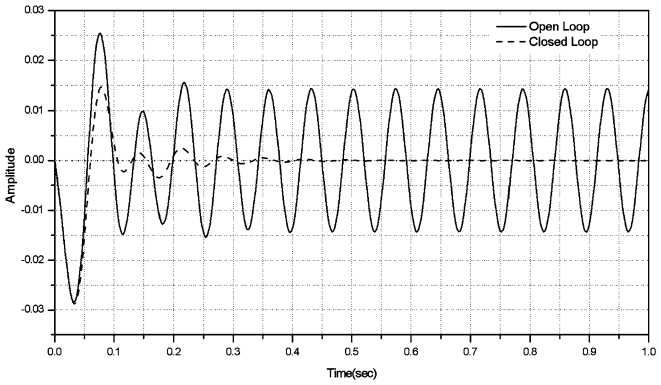

Fig. 7. Time response of the open and closed loop (LQG controller) system.

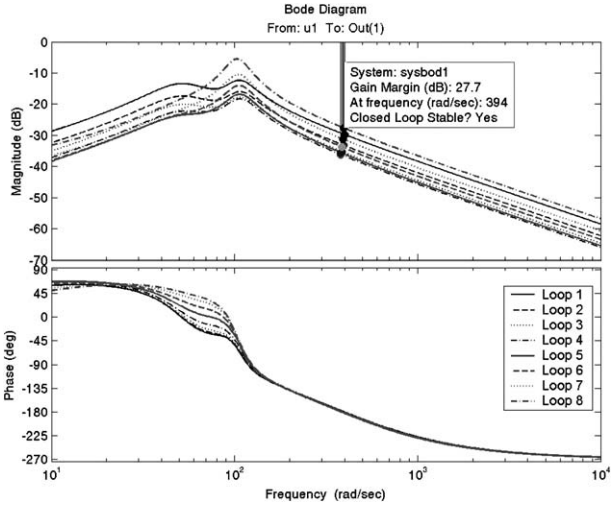

Fig. 8. Loop gain of the individual loops with all except one loop closed at a time.

The LQG controller is designed at the flutter velocity of 44.13 m/s estimated at sea level condition for the active plate. Typical impulse response from disturbance point f_d to observation point w with open and closed loop is shown in the Fig. 7. It is seen from the responses that the system is neutrally stable in the open loop condition. The closed loop system results in a successful suppression of the oscillations. In Fig. 8, the loop gains are shown with all except one control loop closed at a time. The control loop is broken at each actuator input point with the remaining loops closed. There are eight actuators, resulting in eight such loop gains. The gain margin is seen to be around 28 dB in each loop with infinite phase margin. In this calculation the system delay has been approximated by a first order Pade approximation. Figs. 7 and 8 demonstrate that it is possible to use a MIMO feedback controller to achieve a stable flight at the open loop flutter velocity.

In order to determine the enhancement in flutter velocity, the root locus of the closed loop system is plotted as a function of flight velocity from 44.13 to 60 m/s (refer to Fig. 9). It is seen that the system becomes unstable in closed loop at higher velocity. Careful examination of the closed loop response shows that the system looses stability at a speed of 55.5 m/s. Thus, the flutter enhancement is of the order of 25%.

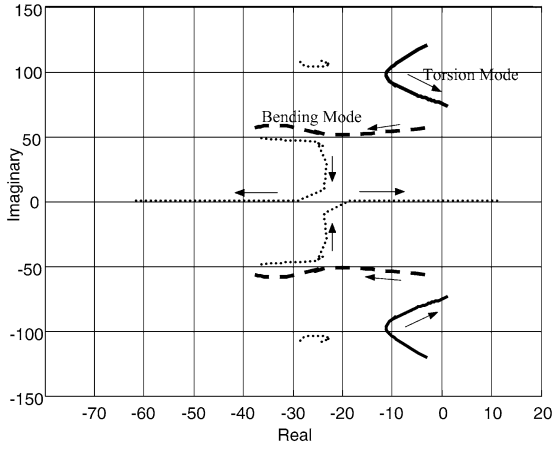

Fig. 9. Root Locus of the closed loop system with increasing forward speed from 44.13 to 60 m/s.

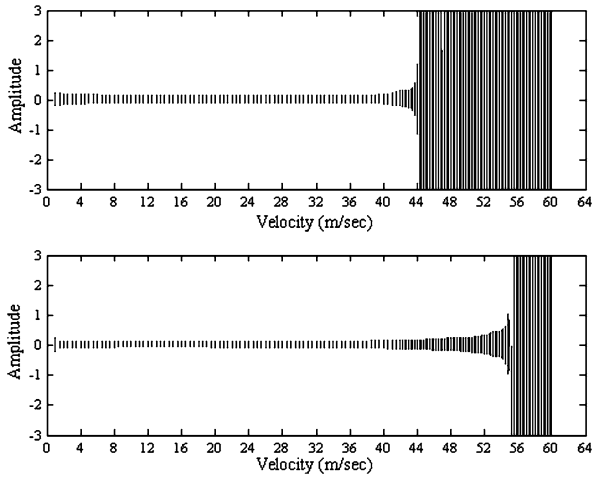

Fig. 10. Open and closed loop responses to a band limited disturbance.

The velocity versus response amplitude plot in Fig. 10 shows clearly that the divergent oscillation onset point has been shifted from 44.13 to 55.5 m/s. These responses have been generated by injecting a band limited white noise at the disturbance input point 'f_d'. The magnitude of this disturbance is fixed based on the typical open loop sensor response level of 150 millivolts as seen at a speed of 40 m/s in the wind tunnel experiments [20] to a similar plate wing model. It is seen that the voltage levels of the sensors and actuators is well within their maximum ranges even when the system is close to the verge of close loop instability.

7. Conclusions

A simplified numerical approach has been presented to develop active flutter control scheme for lifting surfaces. The numerical scheme has employed coupled piezoelectric finite element model, unsteady aerodynamics and Linear Quadratic Gaussian control concept in modal domain to formulate a state-space mathematical model. Multi-Input-Multi-Output feedback controller has been designed, considering multilayered piezoelectric actuators and sensors in closed loop configuration. With the help of a flutter enhancement controller, it has been shown on a composite plate that the flutter speed can be significantly improved using the distributed piezoelectric actuation energy. It has been found that the closed loop system shows an abrupt transition from a stable to unstable state beyond 55.5 m/s. Thus it accounts for a 25% enhancement in the flight envelope. Multi layered bender actuators are appeared to be efficient in aeroelastic control applications than single layer crystal and do not demand more power like stack actuators. Therefore, they can be employed in an integrated form to develop active lifting surfaces for real time applications.

References

[1] H. Horikawa, E.H. Dowell, An elementary explanation of the flutter mechanism with active feedback controls, J. Aircraft 16 (4) (1979) 225–232.
[2] C. Hwang, E.H. Johnson, W.S. Pi, Recent development of the YF-17 active flutter suppression system, J. Aircraft 18 (7) (1981) 537–545.
[3] P.R. Peloubet Jr., R.L. Haller, R.M. Bolding, F-16 flutter suppression system investigation feasibility study and wind tunnel tests, J. Aircraft 19 (2) (1982) 169–175.
[4] E. Nissim, Flutter suppression using active controls based on the concept of aerodynamic energy, NASA TN D-6199, 1971.
[5] R. Freymann, New simplified ways to understand the interaction between aircraft structure and active control systems, AIAA Paper 84-1868, 1984.
[6] M.G. Lyons, R. Vepa, S.C. McIntosh, D.B. Debra, Control law synthesis and sensor design for active flutter suppression, in: Guidance and Control Conference, Key Biscayne, FL, American Institute of Aeronautics and Astronautics, 1973, AIAA Paper No 73-832.
[7] J.W. Edwards, Unsteady aerodynamic modelling and active aeroelastic control, NASA CR-148019, 1977.
[8] J.R. Newsom, Active flutter suppression synthetic using optimal control theory, MS Thesis, The George Washington Univ., 1978.
[9] J.R. Newsom, A method for obtaining practical flutter – suppression control laws using results of optimal control theory, NASA TP 1471, 1979.
[10] V. Mukhopadhyay, J.R. Newsom, I. Abel, Reduced-order optimal feedback control law synthesis for flutter suppression, J. Guidance Control Dynamics 5 (4) (1982) 389–395.
[11] C. Nam, Y. Kim, Optimal design of composite lifting surface for flutter suppression with piezoelectric actuators, AIAA J. 33 (10) (1995) 1897–1904.
[12] J.M. Barker, G.J. Balas, P.A. Blue, Gain-scheduled linear fractional control for active flutter suppression, J. Guidance Control Dynamics 22 (4) (1999) 507–512.
[13] P.P. Friedmann, E. Presente, Active control of flutter in compressible flow and its aeroelastic scaling, J. Guidance Control Dynamics 24 (1) (2001) 167–175.
[14] J.R. Newsom, Designing active control laws in a computational aeroelasticity environment, PhD Thesis, The Virginia Polytechnic Institute and State University, 2002.
[15] J. Heeg, Analytical and experimental investigation of flutter suppression by piezoelectric actuation, NASA TP 3241, 1993.
[16] F. Döngi, D. Dinkler, B. Kröplin, Active panel flutter suppression using self-sensing piezo actuators, AIAA J. 34 (6) (1996) 1224–1230.
[17] S. Raja, et al., Influence of one and two dimensional piezoelectric actuation on active vibration control of smart panels, Aerospace Science and Technology 6 (2002) 209–216.
[18] R. Sreedeep, S. Raja, A.A. Pashilkar, Active flutter suppression of composite wing model using piezo-electric actuators, in: Third International Conference on Theoretical, Applied, Computational and Experimental Mechanics, IIT, Kharagpur, India, 2004.
[19] B. Hassibi, T. Kailath, Mixed least-mean square/H^{∞}-optimal adaptive filtering, in: Thirteenth Asilomar Conference on Signals, Systems and Computers, Pacific Grove, CA, USA, 1996.
[20] S. Raja, et al., Development of flutter control scheme using smart piezoelectric devices on typical aeroelastic wing model, NAL, Bangalore, India, NAL-SP-0510, NAL, 2005.